JCB Article

Myelin-associated glycoprotein and myelin galactolipids stabilize developing axo-glial interactions

Jill Marcus,[1,2] Jeffrey L. Dupree,[1,5] and Brian Popko[1,2,3,4]

[1]UNC Neuroscience Center, [2]Curriculum in Neurobiology, [3]Department of Biochemistry and Biophysics, [4]Program in Molecular Biology and Biotechnology, and [5]Department of Pathology and Laboratory Medicine, University of North Carolina at Chapel Hill, Chapel Hill, NC 27599

We have analyzed mice that lack both the myelin-associated glycoprotein (MAG) and the myelin galactolipids, two glial components implicated in mediating axo-glial interactions during the myelination process. The single-mutant mice produce abnormal myelin containing similar ultrastructural abnormalities, suggesting that these molecules may play an overlapping role in myelin formation. Furthermore, the absence of the galactolipids results in a disruption in paranodal axo-glial interactions, and we show here that similar, albeit less severe, abnormalities exist in the developing MAG mutant. In the double-mutant mice, maintenance of axo-glial adhesion is significantly more affected than in the single mutants, supporting the overlapping function hypothesis. We also show that independently of MAG, galactolipids, and paranodal junctional components, immature nodes of Ranvier form normally, but rapidly destabilize in their absence. These data indicate that distinct molecular mechanisms are responsible for the formation and maintenance of axo-glial interactions.

Introduction

Continuous adhesive contacts between the myelin sheath and the axon are of critical importance to nerve function. Myelin essentially serves as an insulator for neuronal membranes and, as such, is needed for rapid and efficient nerve impulse conduction. Internodal myelinated axon segments are periodically separated by unmyelinated nodes of Ranvier where voltage-gated sodium channels aggregate. It is within these restricted nodal sites where the electrical activity of fibers are processed (Rosenbluth, 1999). The paranodal region flanks the node and is distinctive in appearance in that the cytoplasm is retained within the successive membrane layers forming glial (or paranodal) loops. Paranodal loops terminate in tight association with the engaged axon, and analysis of this membrane interface reveals the presence of transverse bands, electron-dense structures that span the periaxonal space and thus appear to anchor glial loops to the axolemma (Rosenbluth, 1995). The specialized paranodal domain separates the node of Ranvier from the juxtaparanode, the proximal segment coinciding with compacted myelin.

Myelin sheath development also regulates the organization of functional domains within the axolemma (Arroyo et al., 2001). For example, the cell recognition protein contactin-associated protein (Caspr), or paranodin, redistributes to the paranode during myelination (Einheber et al., 1997; Menegoz et al., 1997; Peles et al., 1997). Also, the delayed rectifier potassium (K^+) channels Kv1.1 and Kv1.2 become confined to the juxtaparanode (Wang et al., 1993; Rasband and Shrager, 2000). These K^+ channels associate with Caspr2, a transmembrane protein that is related to, but does not normally localize with, Caspr (Poliak et al., 1999). It is clear that the segregation of these proteins is largely determined by specialized contacts with myelinating cells, because mutant mice with compromised axo-glial junctions also exhibit abnormal protein distributions within the axolemmal membrane (Dupree et al., 1999; Bhat et al., 2001; Boyle et al., 2001).

The search for glia-specific molecules that explicitly direct early neuron-glia interactions has not yet yielded any single strong candidates. Myelin-associated glycoprotein (MAG),* a minor constituent of myelin, is a member of the immunoglobulin gene superfamily of cell recognition proteins (Salzer et al., 1987), and has been characterized as a possible early mediator of axo-glial interactions (Schachner and Bartsch,

Address correspondence to Dr. Brian Popko, The Jack Miller Center for Peripheral Neuropathy, The University of Chicago, 5841 S. Maryland Ave., MC2030, Chicago, IL 60637-1470. Tel.: (773) 702-4953. Fax: (773) 702-9076. E-mail: bpopko@neurology.bsd.uchicago.edu

Key words: myelination; MAG; galactolipids; periaxon; nodes

*Abbreviations used in this paper: Caspr, contactin-associated protein; CGT, ceramide galactosyltransferase; CNS, central nervous system; GalC, galactocerebroside; MAG, myelin-associated glycoprotein; PNS, peripheral nervous system.

2000). MAG is detected on processes during initial stages of axon ensheathment, and is subsequently localized within the periaxonal aspects of fibers (Bartsch et al., 1989; Trapp et al., 1989). MAG-null mutant mice were generated to verify their role in establishing neuron-glia contacts in vivo, but their absence had only minimal effects on myelin formation (Li et al., 1994; Montag et al., 1994).

The myelin galactolipids galactocerebroside (GalC) and its sulfated form sulfatide were also considered to be initiators of myelin formation (Dyer, 1993; Dupree et al., 1998c). Galactolipids are abundantly expressed on the extracellular surface of myelinating membranes, and like MAG, are expressed early during glia differentiation (Raff et al., 1978; Ranscht et al., 1982; Schaeren-Wiemers et al., 1995). The enzyme UDP-galactose:ceramide galactosyltransferase (CGT) converts ceramide to GalC (Morell and Radin, 1969), and both GalC and sulfatide expression are abolished when the enzyme is genetically mutated in mice (Bosio et al., 1996; Coetzee et al., 1996). Like the MAG mutant, myelination is not dramatically inhibited in galactolipid-deficient mice. However, the CGT mutants exhibit a progressive neuropathological phenotype and die prematurely. Ultrastructural pathologies include defects in axo-glial adhesion that likely contribute to the observed nerve conduction delays in the central nervous system (CNS) (Bosio et al., 1996; Coetzee et al., 1996). Specifically, transverse bands do not form, paranodal loops are disoriented, and glial end processes at the node are occasionally mispaired (Dupree et al., 1998a).

Interestingly, the CNS of both MAG and CGT mutants contains common defects that reflect generalized complications in axo-glial adhesion/recognition. For example, there is about a threefold increase in the number of unmyelinated processes (Bartsch et al., 1997; Marcus et al., 2000), some axons are multiply myelinated (Bartsch et al., 1995; Dupree et al., 1998b), and internodal myelin segments can overlap causing nodes to be covered (Bartsch et al., 1995; Dupree et al., 1998a).

The proposed functions ascribed to MAG and the galactolipids do not strongly correlate to the comparatively subtle pathologies induced by their elimination in vivo, yet the two mutant models share several abnormalities, suggesting that they functionally overlap. This study was designed to determine whether MAG- and CGT-derived molecules possess compensating activity. The two single-mutant lines were interbred to generate mice that lack both MAG and galactolipids. The double mutants display a much more severe phenotype, and our results confirm that there is parallel functioning between the membrane components, as their elimination rapidly leads to increased periaxonal process splitting. The study also demonstrates that the abnormalities found in CGT- and CGT/MAG-deficient paranodes are not nearly as prominent earlier in development. This is the first report describing that node of Ranvier formation and maintenance are controlled by distinct molecular mechanisms.

Results

Phenotype of MAG/CGT double mutants

The CGT mutant displays a tremoring phenotype starting at ~2 wk of age. This escalates by 60 d to encompass progressive hindlimb weakness which worsens and eventually leads to total immobility (Coetzee et al., 1996). Most of the CGT mutants die prematurely by ~90 d (Dupree et al., 1998c). In contrast, the MAG mutants do not exhibit an abnormal behavioral phenotype and retain a normal life expectancy (Montag et al., 1994). The MAG/CGT double mutants have a more obvious tremor and unstable gait as

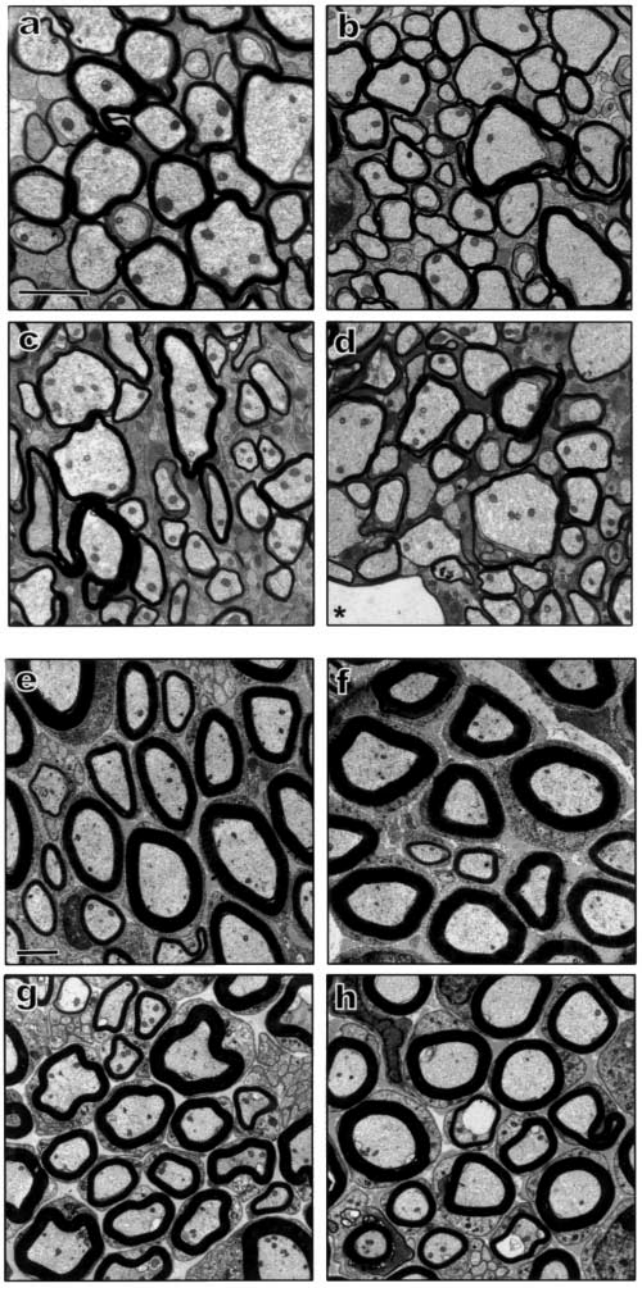

Figure 1. **Ultrastructure of myelinated axons at day 23.** Transverse sections taken from the ventral funiculi of cervical spinal cords of (a) wild-type; (b) $Mag^{-/-}$; (c) $Cgt^{-/-}$; and (d) $Mag^{-/-}Cgt^{-/-}$ mice, and sciatic nerves of (e) wild-type; (f) $Mag^{-/-}$; (g) $Cgt^{-/-}$; and (h) $Mag^{-/-}Cgt^{-/-}$ mice. CNS myelination profile is comparable among the mutants except for vacuolar indication in $Mag^{-/-}Cgt^{-/-}$ tissue (*). PNS myelination appears similar among genotypes with axo-glial splitting noted in some $Cgt^{-/-}$ and $Mag^{-/-}Cgt^{-/-}$ fibers. Bars, 2 μm.

compared with the $Cgt^{-/-}$ mice by day 12. Clinically, the double mutants undergo a more rapid decline culminating in complete hindlimb paralysis with very minimal locomotor activity by postnatal day 21. Mean life expectancy for the CGT mutants is 85.5 d ($n = 12$), compared with the $Mag^{-/-}Cgt^{-/-}$ mutants whose life expectancy is signficantly reduced (mean = 22.2 d, $n = 76$).

Myelination in the $Mag^{-/-}Cgt^{-/-}$ nervous system

In the CNS of MAG and CGT single-mutant mice it has been reported that myelination of axons is mildly abnormal, with processes displaying hypomyelination and more unmyelinated axons (Coetzee et al., 1996; Bartsch et al., 1997; Bosio et al., 1998; Marcus et al., 2000). Given that the $Mag^{-/-}Cgt^{-/-}$ mutants have a more debilitating clinical phenotype and die much earlier, we initially examined if the simultaneous elimination of both gene products causes a more severe disruption to myelin formation. Electron micrographic analysis of transverse sections through 23-d spinal cords shows morphologically intact myelin sheaths in the $Mag^{-/-}Cgt^{-/-}$ mutant, and ultrastructurally, the sheaths resembled those seen in either the $Mag^{-/-}$ or $Cgt^{-/-}$ tissue (Fig. 1). The periodicity and thickness of the double-mutant myelin did not markedly differ from the single mutants, although in some larger diameter fibers, intramyelinic disorganization was apparent. The peripheral nervous system (PNS) of developing CGT- and MAG-deficient mice is not nearly as affected as their CNS (Montag et al., 1994; Dupree et al., 1998b) Similarly, the double-mutant PNS displayed structurally normal, compact myelin with no obvious changes in fiber organization (Fig. 1 h).

We also compared the extent of myelination in the mutants. In the CNS, there was no further significant increase, relative to the single mutants, in the number of unmyelinated processes in $Mag^{-/-}Cgt^{-/-}$ spinal cord; similarly, in the PNS, no difference was found (Table I). We have reported that in the CGT mutant, a transient period of axo-glial splitting occurs in the PNS (Dupree et al., 1998b). Through morphometric quantitation it was determined that this abnormality was not compounded in the $Mag^{-/-}Cgt^{-/-}$ background (Fig. 1, g–h; Table I).

Periaxonal structural defects in MAG/CGT mutant

We previously described that intramyelin vacuolation of larger $Cgt^{-/-}$ spinal cord fibers begins around day 24, and that its incidence dramatically increases with age (Coetzee et al., 1996). Light and electron microscopic analysis revealed that by day 23, $Mag^{-/-}Cgt^{-/-}$ spinal cords exhibited prominent vacuoles within myelinated fibers (Figs. 1 d and 2). Splitting in the majority of these fibers occurred in the periaxonal region (Fig. 2 b). A quantitative analysis was done to compare the frequency of intramyelin and periaxonal splitting in the CGT and double mutants; no such splitting patterns were evident in age-matched wild-type or MAG knock-out tissues. No significant difference was found in the number of mutant axons expressing splitting within compact myelin (Table I). By contrast, the number of fibers displaying splitting along the periaxonal border was over eightfold higher in the MAG/CGT mutants, indicating that axo-glial adhesion is preferentially compromised during development.

Given the intercellular splitting at the periaxon, a morphometric study was conducted to examine its ultrastructure in intact double-mutant fibers. It has been published that this space is unaltered in the MAG mutant optic nerve (Montag et al., 1994), but another study found some of these fibers to have enlargements in the spacing (Li et al., 1994). Here, a sample fiber population was surveyed for the presence of a periaxonal space that spanned at least 50% of

Table I. **Morphometric quantitation of mutant myelin**

	WT	$Mag^{-/-}$	$Cgt^{-/-}$	$Mag^{-/-}Cgt^{-/-}$	*P*
Myelinated processes					
CNS (*n*)	3	3	4	4	
# fibers	830	1,112	1,786	1,702	
% unmyelinated	26.48 ± 1.9	35.85 ± 2.8	41.25 ± 2.4*	41.47 ± 3.2*	*<0.05
PNS (*n*)	2	3	3	3	
# fibers	971	869	1,1019	1,384	
% unmyelinated	58.60 ± 7.1	60.30 ± 7.6	58.59 ± 2.1	60.33 ± 8.1	NS
CNS myelin integrity					
Myelin splitting (*n*)	3	3	4	4	
# myelinated fibers	245	187	549	511	
Intramyelin (%)	ND	ND	1.64 ± 1.1	1.76 ± 0.53	NS
Periaxonal (%)	ND	ND	0.73 ± 0.6	6.26 ± 1.8*	*<0.03
Periaxonal space (*n*)	3	3	3	3	
# myelinated fibers	325	196	180	179	
% fibers presenting	94.2 ± 1.2	80.6 ± 3.4*	91.2 ± 3.1	11.7 ± 1.3*	*<0.05
PNS myelin integrity					
Myelin splitting (*n*)	3	3	3	3	
# fibers	378	345	422	549	
Periaxonal (%)	2.14 ± 1.0	0.88 ± 0.56	10.46 ± 2.6*	10.46 ± 1.7*	*<0.05

Cross sections through 23-d cervical spinal cord and sciatic nerve were electron microscopically analyzed at 10,000 and 6,300×, respectively. Number of fibers sampled per category and mean percentage values ± SEM are noted. Percentages of unmyelinated axons were determined for CNS and PNS fibers. Intramyelinic splitting and splitting at the axo-glial border were quantified in the CNS of $Cgt^{-/-}$ and $Mag^{-/-}Cgt^{-/-}$ genotypes, but were not detected in wild-type and $Mag^{-/-}$ samples (ND). Periaxonal splitting frequency was also determined for PNS fibers. CNS processes were monitored for the presence of a regular periaxonal space that traversed at least half of the fiber diameter. Significance of differences was assessed by a one-way analysis of variance. *n*, number of animals examined; NS, $P > 0.05$.

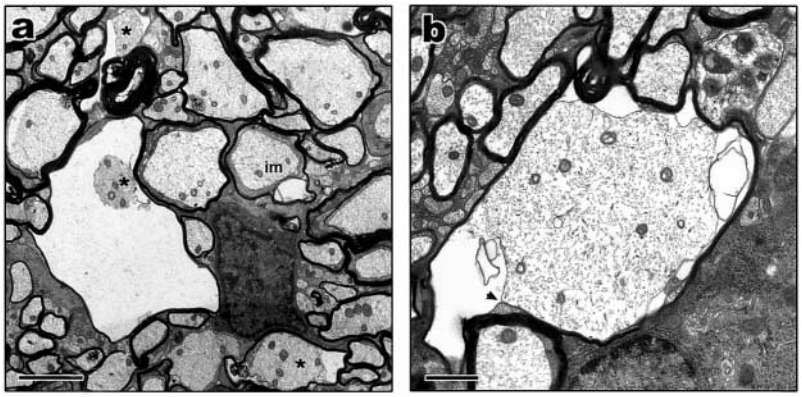

Figure 2. **Periaxonal splitting in MAG/CGT deficient CNS.** Electron micrographs of the ventral column in 23 d $Mag^{-/-}Cgt^{-/-}$ spinal cord. (a) Fibers containing vacuoles around the axon are denoted by an asterisk and fiber exemplifying intramyelin splitting is labeled im. (b) Higher magnification of affected myelin-axon membrane boundary in a vacuolated fiber (arrowhead). Bars: (a) 2 μm; (b) 1 μm.

the fiber perimeter. The majority of wild- type, $Mag^{-/-}$, and $Cgt^{-/-}$ fibers displayed a well-formed, easily identifiable periaxonal space of predicted distance (Fig. 3). There was a slight significant increase in the number of $Mag^{-/-}$ processes displaying reduced periaxonal spacing (Table I). Abnormalities in the periaxonal space were more pronounced in the MAG/CGT mutant where the spacing is noticably absent or irregular in appearance (Fig. 3 d). There was a significant eightfold decrease in the percentage of processes displaying a normal periaxonal gap, further supporting the conclusion that periaxonal cell–cell interactions are specifically affected in the double mutant.

Increased severity of nodal abnormalities in $Mag^{-/-}Cgt^{-/-}$ CNS

We have shown that in the $Cgt^{-/-}$ CNS, the node of Ranvier is structurally compromised, owing to the defective interactions between the oligodendrocyte and the axon (Dupree et al., 1998a). This weakened interaction is believed to deteriorate with age, thus leading to the extensive demyelination of motor neurons in older mutants. To the extent that MAG and the galactolipids appeared to cocontribute to the stabilization of internodal axo-glial contacts, it was of relevance to focus on the ultrastructure of the $Mag^{-/-}Cgt^{-/-}$ paranode, particularly because MAG also localizes to paranodal loops (Bartsch et al., 1989). We found that abnormalities at the node of Ranvier were greatly exacerbated in $Mag^{-/-}Cgt^{-/-}$ tissue at 23 d (Fig. 4). Normally, paranodal loops are sequentially ordered in parallel along the axonal surface as seen in the wild-type and MAG mutant fibers, but this characteristic organization is disrupted in the absence of the galactolipids resulting in variant node length and reduced adhesivity between glial loops and the axolemma. MAG/CGT mutant paranode structure routinely appeared

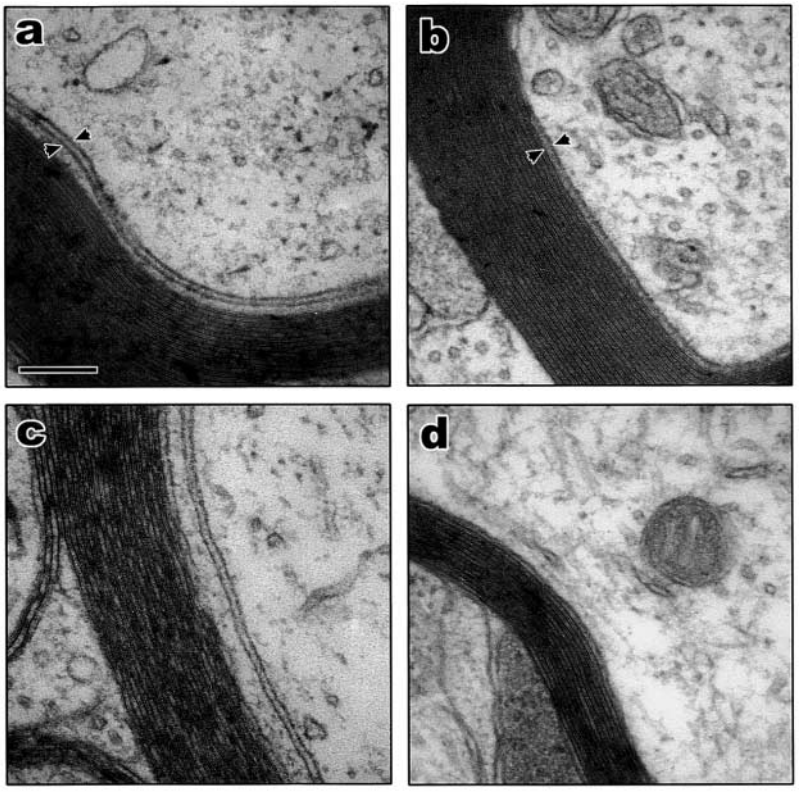

Figure 3. **Defective periaxonal spacing in $Mag^{-/-}Cgt^{-/-}$ mutants.** Myelinated axons of (a) wild-type; (b) $Mag^{-/-}$; (c) $Cgt^{-/-}$; and (d) $Mag^{-/-}Cgt^{-/-}$spinal cords were surveyed for a uniform periaxonal space. Normally formed periaxonal spaces are seen in all genotypes, except for the MAG/CGT mutant. Normal intercellular spacing is highlighted by arrowheads in a and in b, where the MAG mutant lacks a periaxonal cytoplasmic collar. Bar, 200 nm.

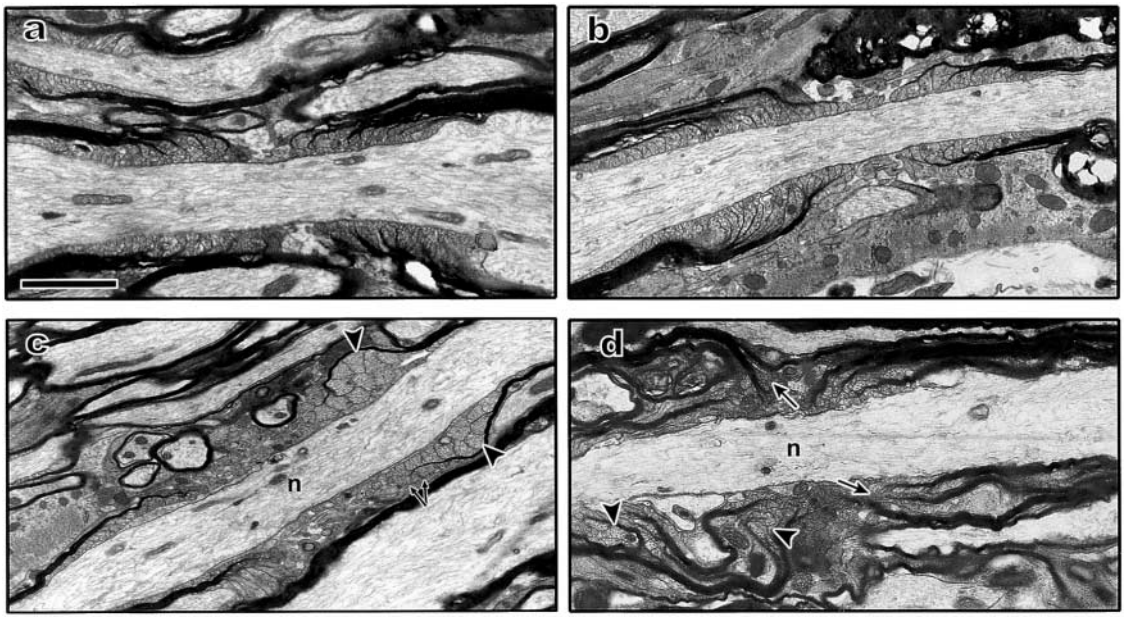

Figure 4. **Comparative electron microscopic analysis of CNS nodal regions.** Longitudinal sections through 23 d (a) wild-type; (b) $Mag^{-/-}$; (c) $Cgt^{-/-}$; and (d) $Mag^{-/-}Cgt^{-/-}$ cervical spinal cord. Node of Ranvier with normal axo-glial junctions seen in wild-type and MAG mutants. (c) Altered paranodal loop organization in littermate CGT mutant. Disordered glial loops oriented in opposing direction (arrows) and not adhering to the ensheathed axon (arrowheads). Nodal gap area appears altered (n). (d) Extensive loss of paranodal axo-glial adhesion in $Mag^{-/-}Cgt^{-/-}$ mutants with indistinct node/paranode structural boundaries. Splitting within paranodal myelin (arrows) and grossly perturbed glial loop–axon interactions (arrowheads) depict early structural breakdown around node region (n). Bar, 2 μm.

more unstable at this age with little apparent interactions between the glial loops and axon (Fig. 4 d). Additionally, the reduction in well defined axo-glial interactions also coincided with general myelin instability at the paranode making identification of nodes very difficult.

Although node/paranode organization in the PNS is much less affected in the CGT mutant, MAG is enriched in the paranodal glial compartments of sciatic nerve fibers (Martini and Schachner, 1986), so we examined this region in the double mutant. Other than the lack of transverse band formation which has previously been reported for the CGT mutant (Dupree and Popko, 1999), nodal and paranodal structures of the sciatic nerve did not display overt abnormalities.

Delayed maturation of nodal regions in the MAG mutant CNS

In the course of analyzing CNS node ultrastructure, we observed that a minority of $Mag^{-/-}$ paranodes exhibited reversed glial loops similar to, though not as extensive as, the CGT mutant (Dupree et al., 1998a). This abnormality occurred in ~20% of the nodes sampled, a lower level compared with the 80% estimate calculated for age-matched CGT mutants (Dupree et al., 1998a). We further characterized the $Mag^{-/-}$ paranodal junctions and found that transverse bands were absent in 23-d MAG mutants, but were evident in age-matched control tissue (Fig. 5, b and c). It is noted that MAG elimination does not result in a severe or progressive phenotype, and that there are no profound ultrastructural abnormalities detected in 2-mo-old mutant paranodes (Montag et al., 1994). Therefore, we examined the possibility that the $Mag^{-/-}$ node–paranode complex matures less efficiently. In fact, transverse bands were observed in some MAG mutant fibers at postnatal day 35 (Fig. 5 d), as well as in 6-mo tissue samples. Correspondingly, there was no increase in the frequency or severity of altered glial loop organization in the older sampling of MAG mutants, indicating that the axo-glial junction develops at a slower rate but does not result in gross structural abnormalities.

In maturing axons, intracellular segregation of the paranodal protein Caspr from the juxtaparanodal domain where Caspr2 and K^+ channel Kv1.1 reside is dependent upon intact axo-glial junctional components (Dupree et al., 1999; Bhat et al., 2001; Poliak et al., 2001). As Fig. 5 e illustrates, Caspr and Caspr2 inhabit adjacent but separate domains along the axon membrane corresponding to the paranode and juxtaparanode, respectively. However, in the MAG mutant, Caspr staining appeared less defined and was more diffuse throughout the processes. More obviously, Caspr2 labeling was not localized to the juxtaparanode, and in some cases could be seen overlapping with paranodal Caspr immunoreactivity (Fig. 5 f). Similarly, juxtaparanodal Kv1.1 localization in wild-type fibers is clearly separated from the nodal Na^+ channel clusters by a small gap that corresponds to the paranodal axolemma. This domain patterning was also disrupted in the MAG mutant; Kv1.1 staining had a more diffuse distribution that extended through the paranodal region to adjoin with the Na^+ channel labeled border (Fig. 5, g–h). An Na^+/K^+ channel double-labeling reaction was performed on MAG mutant tissue aged 7 mo. Most mutant paranodes exhibited a normal distribution of the two axolemmal proteins (inset). These protein localization findings correlate well with the ultrastructural evidence showing that in the absence of MAG the paranodal axo-glial junction experiences delayed maturation.

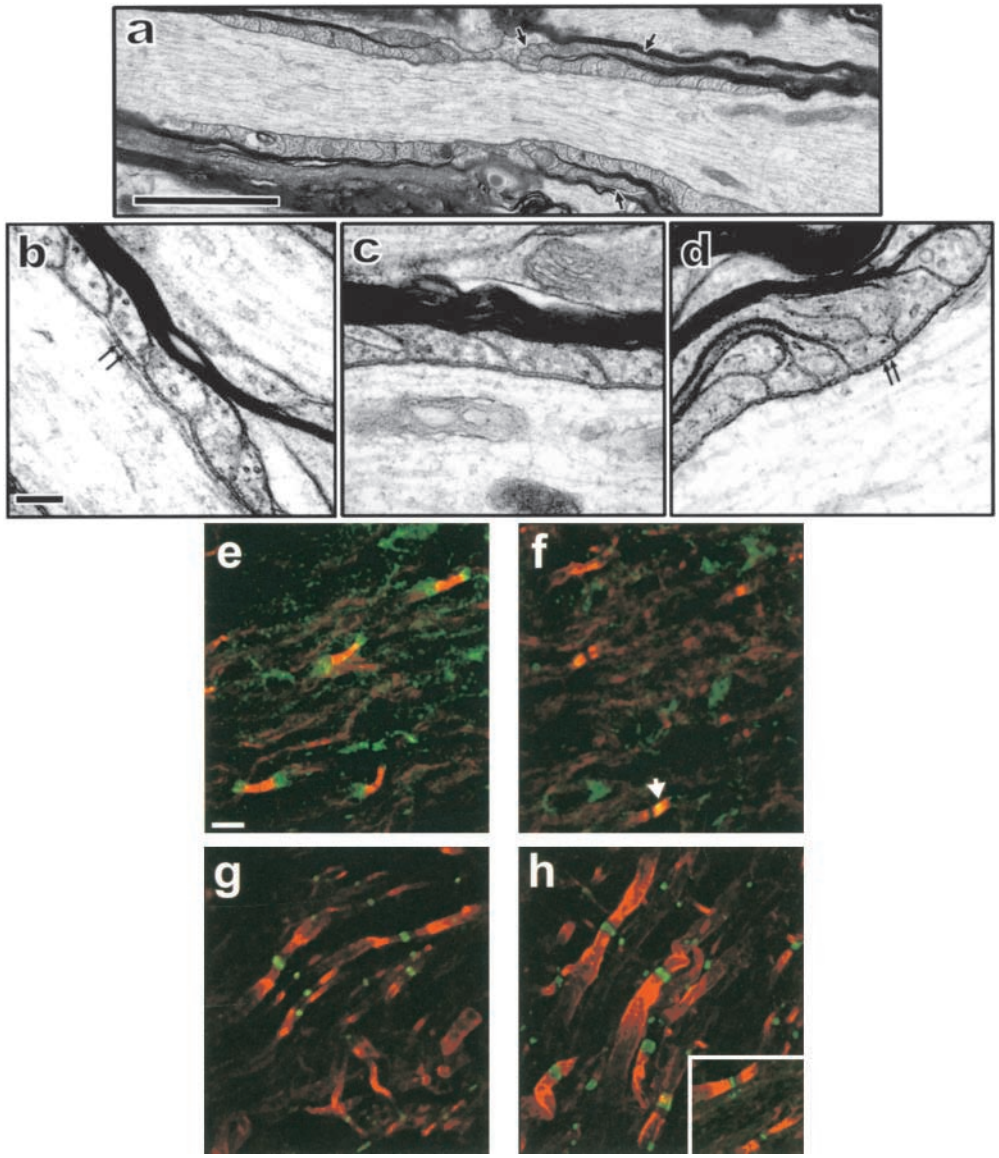

Figure 5. **Characterization of delayed paranode development in MAG deficient CNS.** (a) Electron micrograph of 23-d $Mag^{-/-}$ node displaying everted paranodal loops (arrows). (b) Transverse bands forming in 23-d wild-type (arrows) but not in age-matched $Mag^{-/-}$ spinal cord processes (c). Transverse bands in MAG mutant junctions at day 35 (d, arrows). Double immunocytochemical localization of paranodal and juxtaparanodal axonal proteins Caspr (red) and Caspr2 (green). Compared with wild-type fibers (e), Caspr is not as well localized within the $Mag^{-/-}$ paranode and Caspr2 is absent from the juxtaparanode, occasionally abnormally colocalizing with Caspr in the paranode (f, arrowhead). Juxtaparanodal confinement of Kv1.1 (red) is spatially separated from Na^+ channel domains (green) at 23 d (g), but remains diffusely distributed along $Mag^{-/-}$ processes (h). Inset, showing normal K^+ and Na^+ channel distributions in majority of $Mag^{-/-}$ paranodes aged 7 mo. Bars: (a) 2 μm; (b) 0.2 μm; (e) 6.25 μm.

Galactolipid and MAG deficiencies impede node of Ranvier maintanence, not formation

The dramatic consequences of galactolipid and MAG elimination on nodal regions were observed around the life expectancy endpoint for this mutant line. To clarify to what degree these molecules are involved in the initiation of node formation, we examined the ultrastructure of CNS nodes at postnatal day 15. Unexpectedly, we observed that many paranodal regions of the CGT and MAG/CGT mutants were devoid of the recurrent abnormalities described above and were indistinguishable from the wild- type condition (Fig. 6). At day 15, ~10% of wild-type paranodal regions exhibited relatively mild glial loop inversions near the node region; this occurred about twice as frequently in age-matched CGT and MAG single mutants. In the double mutants, ~30% of the paranodes displayed some form of mild alteration in structure at postnatal day 15. For example, similar observations were made with regard to glial loop orientation and occasionally indications of fiber instability were also seen (i.e., splitting of glial processes from the axon), suggesting a tendency for early degeneration (unpublished data). Compared with the 15-d time point, 23-d-old wild-type and MAG mutant paranode ultrastructure was not appreciably changed. By contrast, at day 23, ~80% of CGT

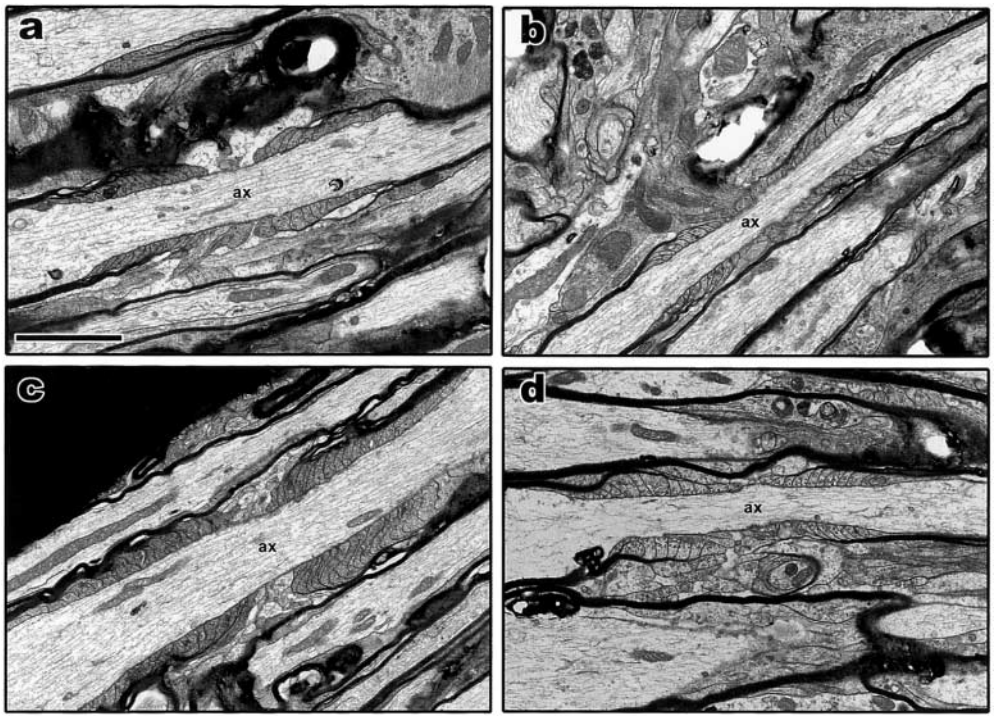

Figure 6. **Paranodal axo-glial interactions establish normally in mutant CNS.** Electron microscopic analysis of 15 d nodal regions in (a) wild-type; (b) $Mag^{-/-}$; (c) $Cgt^{-/-}$; and (d) $Mag^{-/-}Cgt^{-/-}$ ventral column spinal cord fibers. Glial loops surrounding the node form close attachments with the axon (ax) in all genotypes depicted. Paranodal loop positioning and node length in CGT and MAG/CGT mutants are not dramatically altered as they appear at 23 d. Bar, 2 μm.

mutant paranodal regions displayed abnormal axo-glial organization, and all MAG/CGT mutant paranodes examined exhibited significant structural alterations (Fig. 4).

These mutant analyses instruct that nodes of Ranvier are able to form normally, but in the absence of the galactolipids and MAG, the axo-glial interactions rapidly deteriorate between postnatal weeks two and three. We next investigated what other molecular constituents might normally be involved in this multistep process. The junctional space at day 15 was analyzed for the presence of transverse bands in wild-type spinal cord. Transverse bands were not apparent at this time point but were more clearly seen in 23-d-old paranodes (Fig. 7, a–b). Therefore, transverse bands were not coincident with early stages of node formation.

The axonal protein Caspr is believed to be a constituent of the paranodal junction based on an immunoelectron microscopic localization study (Einheber et al., 1997). Furthermore, the elimination of Caspr in mice leads to very similar perturbations in paranode morphology as in the CGT mutant (Bhat et al., 2001). We assessed its intracellular localization in 15- and 23-d-old wild-type fibers to correlate its localization pattern with transverse band formation. As early as day 15, intense Caspr staining appeared to tightly bracket the Na^+ channel clusters in paranodal domains (Fig. 7 c). At day 23, similar, though less restricted, Caspr staining was seen in the MAG mutant and it maintained an immature diffuse pattern in the CGT mutant as shown previously (Dupree et al., 1999) (Fig. 7, e–f).

The only known glial-derived protein that localizes to the paranodal junction is the 155-kD isoform of the neurofascin gene (NF-155). NF-155 codistributes with Caspr during myelination, and it has been speculated that these cell adhesion molecules form interactions at the paranodal junction (Tait et al., 2000; Boyle et al., 2001). To compare the timing of transverse band formation with the localization states of Caspr and NF-155, the same timecourse was examined using an NF-155 antibody. At day 15, NF-155 labeling was partially concentrated around some of the Na^+ channel–positive domains. By 23 d, NF-155 appeared highly concentrated at the paranode, flanking most of the Na^+ channel clusters (Fig. 7, g–h). In the MAG mutant, the NF-155 label concentrated around some Na^+ channel domains but still remained diffusely localized along processes. In $Cgt^{-/-}$ fibers, NF-155 maintained an unconcentrated distribution similar to the axonal staining pattern of Caspr (Fig. 7, i–j). Thus, transverse band formation in the spinal cord correlates to NF-155 concentration within paranodal regions. Additionally, transverse bands and colocalized Caspr/NF-155 are not necessary for the initial positioning of nodes or for establishing attachments between glial loops and the axon.

Discussion

In this study, we have tested for the possibility that MAG and myelin galactolipids function similarly in mediating early stages of myelination. Previous experiments, mainly cell culture based, have employed biochemical strategies to determine that MAG and the galactolipids are critical early mediators of myelin formation (Dupree et al., 1998c; Schachner and Bartsch, 2000). Analyses of the two single-null mutant lines and the MAG/CGT mutant demonstrate that myelina-

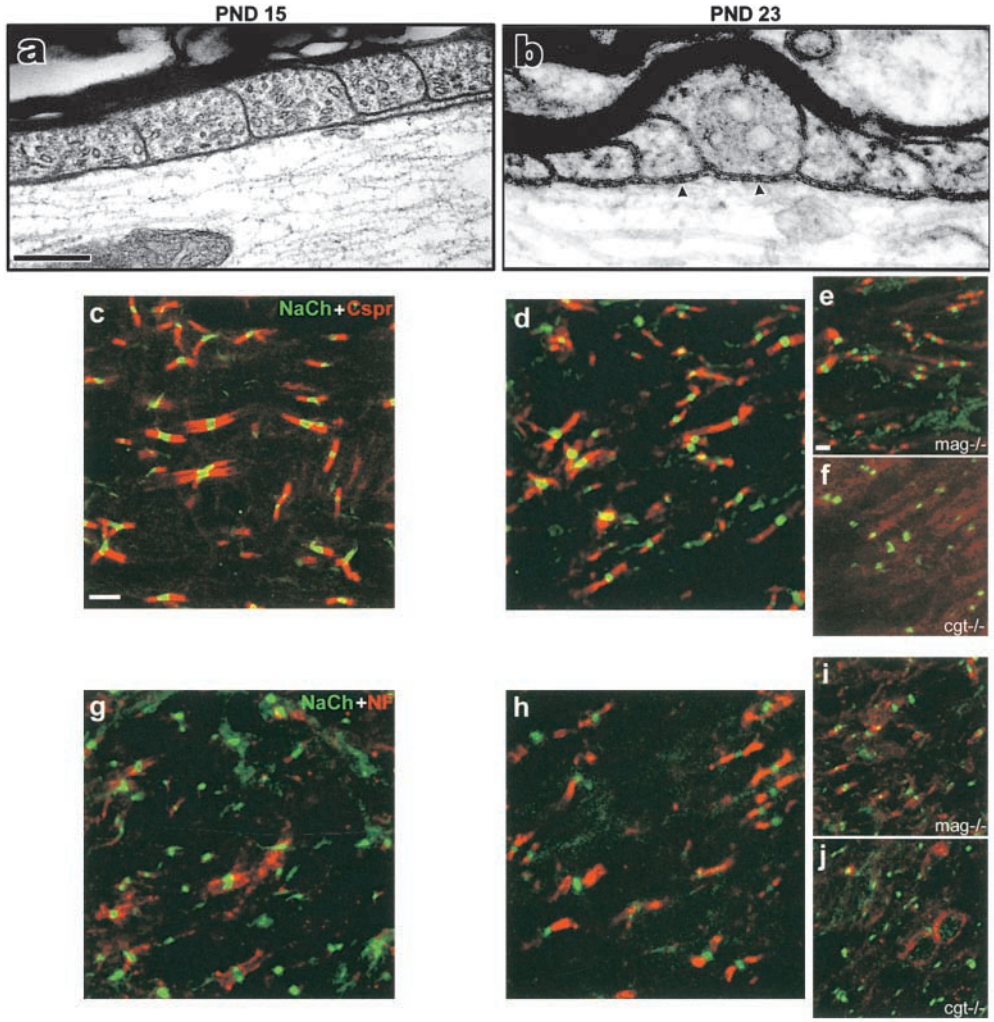

Figure 7. **Normal molecular development of CNS paranodal region.** (a) Electron micrographs of axo-glial junctions reveal that transverse bands are not apparent at postnatal day (PND) 15 but are seen in PND 23 wild-type spinal cord (b, arrowheads). Immunocytochemical staining patterns of paranodal cell adhesion proteins Caspr and NF-155 (red): (c) Caspr (Cspr) is well localized by PND 15 in the normal axolemma surrounding Na^+ channel (NaCh) clusters (green) as it is at 23 d (d). NF-155 (NF), a glial cell component, is not highly concentrated around Na^+ channel domains (green) at PND 15 (g) but becomes rapidly localized to the paranode by PND 23 (h). Caspr and NF-155 are partially localized in most MAG mutant paranodes at 23 d (e and i) but do not distribute to the paranode in $Cgt^{-/-}$ processes (f and j). Nodal Na^+ channels appear segregated in all genotypes. Bars: (a) 0.2 μm; (c and e) 6.25 μm.

tion proceeds independently of both membrane components. However, double elimination of MAG and galactolipids in vivo leads to an accelerated breakdown in CNS axo-glial interactions, demonstrating that they are able to functionally compensate for one another in an intercellular adhesion capacity. Furthermore, the significant increase in periaxonal splitting is accompanied by a lack of a uniform periaxonal space, which further supports that such interactions are fundamentally altered either through a direct molecular spacing mechanism common to both sets of molecules or as the result of ubiquitously distorted interactions between plasma membrane surfaces. The double mutation effect is a relatively specific one, in that further significant disruptions to myelination and overall sheath structure are not seen and oligodendrocytes remain viable (unpublished data). Myelin structures in the double-mutant PNS remain principally intact, a finding that is in line with previous single-mutant studies (Montag et al., 1994; Dupree and Popko, 1999).

A striking observation was that paranodal structural defects are more dramatic in the $Mag^{-/-}Cgt^{-/-}$ mutant at PND 23. Even though MAG and the galactolipids are not enriched in the paranodal region, their concurrent absence exacerbates the paranodal abnormalities of the $Cgt^{-/-}$ background. This may occur because galactolipid-negative paranodal junctions are already weakened, and reduced axo-glial adhesion along the $Mag^{-/-}Cgt^{-/-}$ internode causes deterioration of the paranode earlier. Alternatively, the galactolipids are needed for axo-glial junction interactions, but MAG might also function at the paranode to restrain glial loop attachments, albeit insufficiently to compensate for the loss of the galactolipids in the CGT mutant. Nevertheless, the worsened phenotype and reduced lifespan of the double mutants can readily be accounted for by the conspicuous internodal vacuoles and the reduced paranodal adhesive junctions.

It is not clear how these disparate molecules mediate similar functions. MAG is a sialic acid–binding protein shown to

selectively bind sialylated glycosphingolipids, abundant gangliosides of neuronal cell surfaces (Vyas and Schnaar, 2001). Sulfatides are believed to contribute to cell recognition events during development but as of yet, axonal ligands for the galactolipids have not been found (Vos et al., 1994). Both sulfatide and MAG have been shown to interact with members of the tenascin extracellular matrix protein family, including tenascin-R, perhaps to modulate adhesive properties during myelination (Crossin and Edelman, 1992; Yang et al., 1996; Pesheva et al., 1997). It is also noted that the absence of the abundant galactolipids could indirectly exert effects if it pervasively alters the molecular arrangement within plasma membranes, or through the mistargeting of certain glial cell adhesion proteins via glycolipid-dependent transport mechanisms (Kramer et al., 1997; Bosio et al., 1998). Both cases could potentially impact early myelination processes but do not rule out direct effect mechanisms.

MAG and galactolipids have additionally been characterized as transducing molecules that expedite myelin development in the CNS (Li et al., 1994; Montag et al., 1994; Dupree et al., 1998b; Marcus et al., 2000). Therefore, it was interesting to find that MAG-deficient paranode maturation is delayed. These data illustrate that the functions of the two membrane components diverge at the paranode, as galactolipids are necessary for maintaining the axo-glial interactions, whereas MAG facilitates their development in the CNS.

A most unexpected finding was that the severe paranodal structural abnormalities observed in 23-d CGT and MAG/CGT mutants are either not present or are comparatively mild earlier in development, indicating that paranodal regions initially form normally. It has been reported that transverse bands are a late-developing structure in the rodent paranode (Tao-Cheng and Rosenbluth, 1983). In fact, examination of PND 15 paranodal regions reveals that paranodal loops are able to adhere to the axolemma before transverse bands spanning the intercellular space appear. This suggests that transverse bands function to secure the paranodal axo-glial attachments once they have been established, but that they are not used during early interactions at the paranode.

We have also detailed the early expression sequence of the paranodal cell adhesion proteins Caspr and NF-155 and found that Caspr is localized by day 15 before transverse band formation. By day 23, both restricted NF-155 localization and transverse bands appear. Although the two protein isolates have not been shown to interact (Tait et al., 2000), our results suggest that NF-155 and Caspr are involved in the permanent anchoring of glial loops to the axon, perhaps through the formation of transverse bands. Because both Caspr and NF-155 never localize in the CGT mutant CNS, it is presumed that galactolipids contribute to paranodal axo-glial contact maintenance either through direct interactions with the axon or by regulating the trafficking of NF-155 to cell surfaces, or both. The process by which galactolipids rapidly stabilize the architecture of the paranodal axo-glial junction is reminescent of neuromuscular synapse differentiation where nerve-derived agrin is needed for the early stabilization, but not formation of postsynaptic acetylcholine receptor end-plate complexes (Lin et al., 2001).

The results presented additionally offer insight into sodium channel partitioning within the developing nodal axolemma. Sodium channels cluster normally in the CGT (Dupree et al., 1999) and MAG mutants (Vabnick et al., 1997), and similarly, no change in the number of these clusters was detected in the CGT/MAG double mutants (unpublished data). That sodium channels apparently distribute normally despite overt defects in paranodal axo-glial interactions in the CGT and CGT/MAG mutants was somewhat surprising. Nevertheless, the examination of early CNS paranode development described here indicates that sodium channels cluster within developing nodes with initially normal axo-glial organization in the mutants. It should also be noted that there are at least normal numbers of oligodendrocytes in the CGT (Marcus et al., 2000) and CGT/MAG mutants (unpublished data). Together, these findings may account for normal sodium channel domain appearance within the mutant axons, as essential soluble and contact-mediated glial signals would still be available for the induction and early maintenance of sodium channel clustering (Kaplan et al., 1997, 2001; Peles and Salzer, 2000; Rasband and Shrager, 2000).

Here we extend on the molecular characterization of CNS axo-glial interactions by showing that MAG and the myelin galactolipids functionally overlap with one another in maintaining intercellular adhesion along myelinated axons, and that these molecules act synergistically at the paranode to promote its structural maintenance. Also, we have determined that nodes stably form in the absence of clustered junctional cell adhesion proteins and transverse bands but that these components, possibly acting in complexes, participate in preserving nodal structure long term.

Materials and methods

Generation of MAG/CGT mutant mice

Female CGT heterozygotes were bred with male MAG-null mutants (Li et al., 1994) to obtain offspring double positive for mutant alleles. CGT wild-type and null alleles were identified by PCR screening as previously described (Coetzee et al., 1999). Transmission of the MAG alleles were monitored by PCR amplification of sequences specific for the wild-type allele: JM100243, 5′-AAGATGATATTCCTCGCCACC-3′; JM200243, 5′-CGGAAATAGTATTTGCCTCCC-3′, and for the mutant allele containing neo gene sequence: MAGmut(−), 5′-CGCCTTCTTGACGAGTTCTTCTGA-3′ with forward primer JM200243. All experiments were performed in compliance with the relevant laws and institutional guidelines and were approved by the University of North Carolina's Institutional Animal Care and Use Committee.

Electron microscopy

Anesthetized mice were perfused and postfixed as previously described (Dupree et al., 1998a). Cervical (C3) spinal cord and sciatic nerves were processed and analyzed on a Leo910 electron microscope. Digital images were captured using a Gatan BioScan camera (Model 792) and converted using the Digital Micrograph software package (v. 3.4; Gatan, Inc.).

Statistical analysis

Significant differences between mean values were determined by a one-way analysis of variance. Subsequent comparisons of individual genotypes (Student-Newman-Keuls Multiple Comparisons Test) were conducted using the statistical software program InStat (v. 3.0; GraphPad Software, Inc.).

Immunocytochemistry

Spinal cords (C3) and teased sciatic nerve fiber preps were prepared for fluorescent labeling as previously described (Dupree et al., 1999). Frozen sections were incubated with the following primary antibodies: Sodium channel (mouse monoclonal [Sigma-Aldrich]; rabbit polyclonal/isoform

1.6, a gift from Dr. Rock Levinson, University of Michigan, Ann Arbor, MI); potassium channel Kv1.1 (mouse monoclonal [Upstate Biotechnology]; Caspr/paranodin (rabbit polyclonal, a gift from Dr. Elior Peles, The Weizmann Institute of Science, Rehovot, Israel [Peles et al., 1997]); neurofascin 155 (rabbit polyclonal, gift from Dr. Peter Brophy, University of Edinburgh, Edinburgh, UK [Tait et al., 2000]); and Caspr2 (rabbit monoclonal, a gift from Dr. Elior Peles [Poliak et al., 1999]). Laser scanning confocal images were taken on a Leica TCS-NT microscope. Images were generated using a pinhole setting of 1.0 Airy disc units through the compilation of 16 optical frames at a step size of 0.41 μm.

The authors thank Drs. Rock Levinson, Peter Brophy, and Elior Peles for generously providing antibodies, and Dr. Mechelle Mayleben for her assistance with the statistical analyses.

This work was supported by NIH grant NS27736 (to B. Popko). J. Dupree was supported by a grant from the National M.S. Society.

Submitted: 12 November 2001
Revised: 17 December 2001
Accepted: 19 December 2001

References

Arroyo, E.J., T. Xu, S. Poliak, M. Watson, E. Peles, and S.S. Scherer. 2001. Internodal specializations of myelinated axons in the central nervous system. *Cell Tissue Res.* 305:53–66.

Bartsch, U., F. Kirchhoff, and M. Schachner. 1989. Immunohistological localization of the adhesion molecules L1, N-CAM, and MAG in the developing and adult optic nerve of mice. *J. Comp. Neurol.* 284:451–462.

Bartsch, U., D. Montag, S. Bartsch, and M. Schachner. 1995. Multiply myelinated axons in the optic nerve of mice deficient for the myelin-associated glycoprotein. *Glia.* 14:115–122.

Bartsch, S., D. Montag, M. Schachner, and U. Bartsch. 1997. Increased number of unmyelinated axons in optic nerves of adult mice deficient in the myelin-associated glycoprotein (MAG). *Brain Res.* 762:231–234.

Bhat, M.A., J.C. Rios, Y. Lu, G.P. Garcia-Fresco, W. Ching, M. St Martin, J. Li, S. Einheber, M. Chesler, J. Rosenbluth, et al. 2001. Axon-glia interactions and the domain organization of myelinated axons requires neurexin IV/Caspr/Paranodin. *Neuron.* 30:369–383.

Bosio, A., E. Binczek, and W. Stoffel. 1996. Functional breakdown of the lipid bilayer of the myelin membrane in central and peripheral nervous system by disrupted galactocerebroside synthesis. *Proc. Natl. Acad. Sci. USA.* 93: 13280–13285.

Bosio, A., H. Bussow, J. Adam, and W. Stoffel. 1998. Galactosphingolipids and axono-glial interaction in myelin of the central nervous system. *Cell Tissue Res.* 292:199–210.

Boyle, M.E., E.O. Berglund, K.K. Murai, L. Weber, E. Peles, and B. Ranscht. 2001. Contactin orchestrates assembly of the septate-like junctions at the paranode in myelinated peripheral nerve. *Neuron.* 30:385–397.

Coetzee, T., N. Fujita, J. Dupree, R. Shi, A. Blight, K. Suzuki, and B. Popko. 1996. Myelination in the absence of galactocerebroside and sulfatide: normal structure with abnormal function and regional instability. *Cell.* 86:209–219.

Coetzee, T., K. Suzuki, K.A. Nave, and B. Popko. 1999. Myelination in the absence of galactolipids and proteolipid proteins. *Mol. Cell. Neurosci.* 14:41–51.

Crossin, K.L., and G.M. Edelman. 1992. Specific binding of cytotactin to sulfated glycolipids. *J. Neurosci. Res.* 33:631–638.

Dupree, J.L., and B. Popko. 1999. Genetic dissection of myelin galactolipid function. *J. Neurocytol.* 28:271–279.

Dupree, J.L., T. Coetzee, A. Blight, K. Suzuki, and B. Popko. 1998a. Myelin galactolipids are essential for proper node of Ranvier formation in the CNS. *J. Neurosci.* 18:1642–1649.

Dupree, J.L., T. Coetzee, K. Suzuki, and B. Popko. 1998b. Myelin abnormalities in mice deficient in galactocerebroside and sulfatide. *J. Neurocytol.* 27:649–659.

Dupree, J.L., K. Suzuki, and B. Popko. 1998c. Galactolipids in the formation and function of the myelin sheath. *Microsc. Res. Tech.* 41:431–440.

Dupree, J.L., J.A. Girault, and B. Popko. 1999. Axo-glial interactions regulate the localization of axonal paranodal proteins. *J. Cell Biol.* 147:1145–1152.

Dyer, C.A. 1993. Novel oligodendrocyte transmembrane signaling systems. Investigations utilizing antibodies as ligands. *Mol. Neurobiol.* 7:1–22.

Einheber, S., G. Zanazzi, W. Ching, S. Scherer, T.A. Milner, E. Peles, and J.L. Salzer. 1997. The axonal membrane protein Caspr, a homologue of neurexin IV, is a component of the septate-like paranodal junctions that assemble during myelination. *J. Cell Biol.* 139:1495–1506.

Kaplan, M.R., M.H. Cho, E.M. Ullian, L.L. Isom, S.R. Levinson, and B.A. Barres. 2001. Differential control of clustering of the sodium channels Na(v)1.2 and Na(v)1.6 at developing CNS nodes of Ranvier. *Neuron.* 30:105–119.

Kaplan, M.R., A. Meyer-Franke, S. Lambert, V. Bennett, I.D. Duncan, S.R. Levinson, and B.A. Barres. 1997. Induction of sodium channel clustering by oligodendrocytes. *Nature.* 386:724–728.

Kramer, E.M., T. Koch, A. Niehaus, and J. Trotter. 1997. Oligodendrocytes direct glycosyl phosphatidylinositol-anchored proteins to the myelin sheath in glycosphingolipid-rich complexes. *J. Biol. Chem.* 272:8937–8945.

Li, C., M.B. Tropak, R. Gerlai, S. Clapoff, W. Abramow-Newerly, B. Trapp, A. Peterson, and J. Roder. 1994. Myelination in the absence of myelin-associated glycoprotein. *Nature.* 369:747–750.

Lin, W., R.W. Burgess, B. Dominguez, S.L. Pfaff, J.R. Sanes, and K.F. Lee. 2001. Distinct roles of nerve and muscle in postsynaptic differentiation of the neuromuscular synapse. *Nature.* 410:1057–1064.

Marcus, J., J.L. Dupree, and B. Popko. 2000. Effects of galactolipid elimination on oligodendrocyte development and myelination. *Glia.* 30:319–328.

Martini, R., and M. Schachner. 1986. Immunoelectron microscopic localization of neural cell adhesion molecules (L1, N-CAM, and MAG) and their shared carbohydrate epitope and myelin basic protein in developing sciatic nerve. *J. Cell Biol.* 103:2439–2448.

Menegoz, M., P. Gaspar, M. Le Bert, T. Galvez, F. Burgaya, C. Palfrey, P. Ezan, F. Arnos, and J.A. Girault. 1997. Paranodin, a glycoprotein of neuronal paranodal membranes. *Neuron.* 19:319–331.

Montag, D., K.P. Giese, U. Bartsch, R. Martini, Y. Lang, H. Bluthmann, J. Karthigasan, D.A. Kirschner, E.S. Wintergerst, K.A. Nave, et al. 1994. Mice deficient for the myelin-associated glycoprotein show subtle abnormalities in myelin. *Neuron.* 13:229–246.

Morell, P., and N.S. Radin. 1969. Synthesis of cerebroside by brain from uridine diphosphate galactose and ceramide containing hydroxy fatty acid. *Biochemistry.* 8:506–512.

Peles, E., M. Nativ, M. Lustig, M. Grumet, J. Schilling, R. Martinez, G.D. Plowman, and J. Schlessinger. 1997. Identification of a novel contactin-associated transmembrane receptor with multiple domains implicated in protein-protein interactions. *EMBO J.* 16:978–988.

Peles, E., and J.L. Salzer. 2000. Molecular domains of myelinated axons. *Curr. Opin. Neurobiol.* 10:558–565.

Pesheva, P., S. Gloor, M. Schachner, and R. Probstmeier. 1997. Tenascin-R is an intrinsic autocrine factor for oligodendrocyte differentiation and promotes cell adhesion by a sulfatide-mediated mechanism. *J. Neurosci.* 17:4642–4651.

Poliak, S., L. Gollan, R. Martinez, A. Custer, S. Einheber, J.L. Salzer, J.S. Trimmer, P. Shrager, and E. Peles. 1999. Caspr2, a new member of the neurexin superfamily, is localized at the juxtaparanodes of myelinated axons and associates with K+ channels. *Neuron.* 24:1037–1047.

Poliak, S., L. Gollan, D. Salomon, E.O. Berglund, R. Ohara, B. Ranscht, and E. Peles. 2001. Localization of Caspr2 in myelinated nerves depends on axon-glia interactions and the generation of barriers along the axon. *J. Neurosci.* 21:7568–7575.

Raff, M.C., R. Mirsky, K.L. Fields, R.P. Lisak, S.H. Dorfman, D.H. Silberberg, N.A. Gregson, S. Leibowitz, and M.C. Kennedy. 1978. Galactocerebroside is a specific cell-surface antigenic marker for oligodendrocytes in culture. *Nature.* 274:813–816.

Ranscht, B., P.A. Clapshaw, J. Price, M. Noble, and W. Seifert. 1982. Development of oligodendrocytes and Schwann cells studied with a monoclonal antibody against galactocerebroside. *Proc. Natl. Acad. Sci. USA.* 79:2709–2713.

Rasband, M.N., and P. Shrager. 2000. Ion channel sequestration in central nervous system axons. *J Physiol.* 525 Pt 1:63-73.

Rosenbluth, J. 1999. A brief history of myelinated nerve fibers: one hundred and fifty years of controversy. *J. Neurocytol.* 28:251–262.

Rosenbluth, J. 1995. Glial membranes and axonal junctions. *In* Neuroglia. H. Kettenmann and B.R. Ransom, editors. Oxford University Press, New York. 613–633.

Salzer, J.L., W.P. Holmes, and D.R. Colman. 1987. The amino acid sequences of the myelin-associated glycoproteins: homology to the immunoglobulin gene superfamily. *J. Cell Biol.* 104:957–965.

Schachner, M., and U. Bartsch. 2000. Multiple functions of the myelin-associated glycoprotein MAG (siglec-4a) in formation and maintenance of myelin. *Glia.* 29:154–165.

Schaeren-Wiemers, N., P. van der Bijl, and M.E. Schwab. 1995. The UDP-galactose:ceramide galactosyltransferase: expression pattern in oligodendrocytes and Schwann cells during myelination and substrate preference for hydroxyceramide. *J. Neurochem.* 65:2267–2278.

Tait, S., F. Gunn-Moore, J.M. Collinson, J. Huang, C. Lubetzki, L. Pedraza, D.L. Sherman, D.R. Colman, and P.J. Brophy. 2000. An oligodendrocyte cell adhesion molecule at the site of assembly of the paranodal axo-glial junction. *J. Cell Biol.* 150:657–666.

Tao-Cheng, J.H., and J. Rosenbluth. 1983. Axolemmal differentiation in myelinated fibers of rat peripheral nerves. *Brain Res.* 285:251–263.

Trapp, B.D., S.B. Andrews, C. Cootauco, and R. Quarles. 1989. The myelin-associated glycoprotein is enriched in multivesicular bodies and periaxonal membranes of actively myelinating oligodendrocytes. *J. Cell Biol.* 109:2417–2426.

Vabnick, I., A. Messing, S.Y. Chiu, S.R. Levinson, M. Schachner, J. Roder, C. Li, S. Novakovic, and P. Shrager. 1997. Sodium channel distribution in axons of hypomyelinated and MAG null mutant mice. *J. Neurosci. Res.* 50:321–336.

Vos, J.P., M. Lopes-Cardozo, and B.M. Gadella. 1994. Metabolic and functional aspects of sulfogalactolipids. *Biochim. Biophys. Acta.* 1211:125–149.

Vyas, A.A., and R.L. Schnaar. 2001. Brain gangliosides: Functional ligands for myelin stability and the control of nerve regeneration. *Biochimie.* 83:677–682.

Wang, H., D.D. Kunkel, T.M. Martin, P.A. Schwartzkroin, and B.L. Tempel. 1993. Heteromultimeric K+ channels in terminal and juxtaparanodal regions of neurons. *Nature.* 365:75–79.

Yang, L.J., C.B. Zeller, N.L. Shaper, M. Kiso, A. Hasegawa, R.E. Shapiro, and R.L. Schnaar. 1996. Gangliosides are neuronal ligands for myelin-associated glycoprotein. *Proc. Natl. Acad. Sci. USA.* 93:814–818.